Int. J. Electrochem. Sci., 8 **(2013)** 4206 - 4214

International Journal of
ELECTROCHEMICAL
SCIENCE
www.electrochemsci.org

Electrodeposition of Silicon from 1-butyl-3-methyl-pyridinium bis(triflurometylsulfonyl) imide ionic liquid

Jesik Park[1], *Churl Kyoung Lee*[1,*], *Kyungjung Kwon*[2], *Hansu Kim*[3,*]

[1] School of Advanced Materials & Systems Engineering, Kumoh National Institute of Technology, Gumi, Gyungsangbuk-do 730-701, Republic of Korea
[2] Department of Energy & Mineral Resources Engineering, Sejong University, Seoul 143-747, Republic of Korea
[3] Department of Energy Engineering, Hanyang University, Seoul 133-791, Republic of Korea
[*]E-mail: khansu@hanyang.ac.kr; cklee@kumoh.ac.kr

Received: 2 December 2012 / *Accepted:* 6 February 2013 / *Published:* 1 March 2013

Electrodeposition of silicon on various electrode materials was investigated from a 1-butyl-3-methylpyridinium bis(trifluoromethylsulfonyl) imide([BMPy]Tf_2N) with $SiCl_4$. Linear sweep voltammograms of Au, Al and Cu electrodes showed the possibility of the electrodeposition of elemental Si, while Ag electrode a showed smaller reductive potential window in the same electrolyte composition. We demonstrated that Si thin film could be obtained on the Au electrode by the potentiostatic condition, which was confirmed by various analytical techniques including x-ray photoelectron spectroscopy, x-ray diffraction and scanning electron microscopy with energy dispersive spectroscopy.

Keywords: Room temperature ionic liquid, Electrodepositon, Silicon, 1-butyl-3-methylpyridinium bis(trifluoromethylsulfonyl) imide

1. INTRODUCTION

Electrodeposition of silicon has gained much attention for the production of its thin-film form, widely used in photovoltatic devices, lithium battery anode and opto-electronic devices, since electrochemical deposition enables much simpler and less expensive fabrication processes than high vacuum deposition techniques such as chemical vapor deposition.[1-9] However, elemental silicon film cannot be electrochemically deposited from aqueous electrolyte because silicon has large reduction overpotential and high chemical reactivity with water. To this end, several electrolyte systems for the electrodeposition of Si thin film have been suggested such as high temperature molten salts[8,10] and various organic solvents with silicon halide.[1,2,4,9] However, these methods cannot be employed due to their disadvantages, i.e., high temperature operation for molten salts system and incorporated impurities such as carbon and oxygen from organic solvent system with silicon halide. Recently, room temperature ionic liquids (RTILs) have gained attention as promising non-aqueous electrolytes for the electrodeposition of high quality silicon thin film[3,5,6-7], because RTTL shows high chemical/electrochemical stability even under strongly reducing condition, which enables the electrodeposition of pure silicon thin film[11-13]. Since Abedin et al. first reported that silicon thin film can be obtained in the electrochemical deposition from 1-butyl-1methylpyrrolidinium bis(trifluoromethylsulfonyl) imde([BMP]Tf_2N) with $SiCl_4$ as a Si source[3], many research groups have reported the successful electrodeposition of silicon and its alloy in various forms such as thin film, bulk materials and nanowire.[3,5-6,14-16] In this work, we investigated the electrodeposition of silicon from a room temperature ionic liquid electrolyte system, i.e., 1-butyl-3-methylpyridinium bis(trifluoromethylsulfonyl) imide([BMPy]Tf_2N) with $SiCl_4$. Although the reduction potential of BMPy cation is more positive than that of $SiCl_4$ in the pure [BMPy]Tf_2N ionic liquid, we found the widening of the potential window of [BMPy]Tf_2N with the addition of $SiCl_4$, which enables the successful electrochemical deposition of Si thin film, which was confirmed by various analytical techniques including x-ray photoelectron spectroscopy, x-ray diffraction and scanning electron microscopy with energy dispersive spectroscopy.

2. EXPERIMENTAL

1-butyl-3-methylpyridinium bis(trifluoromethylsulfonly) imide(C-Tri, Korea) was used after vacuum drying at 100 °C for 24 hours and $SiCl_4$ (99.99%, Sigm-Aldrich) was used as received. Foils of Au, Al, Cu and Ag (Sigma-Aldrich) were used as a working electrode and Pt wires were used as both counter and reference electrodes. All electrodes were cleaned with a mixture solution of H_2SO_4 and H_2O_2 (1:1, vol. %) prior to all experiments.

All experiments were carried out in an argon-filled glove box(Korea Ki-Yeon, battery grade, Korea). For linear sweep voltammetry, Au, Al, Cu and Ag foils with the area of 0.126 cm^2 (Au, Al, Cu and Ag) were as a working electrode and Pt wires(2mm in thickness, 50 mm in length) were used as counter and quasi-reference electrode [17, 18] using lab-made Teflon three-electrode systems shown in Fig. 1(a). Potential was scanned with a sweep rate of 10 mVs (vs. Pt quasi-reference electrode) using a potentiostat/galvanostat(Electrochemical interface 1287, Solartron Analytical). Electrochemical impedance spectroscopy was performed using the two electrode cell as shown in Fig. 1(b) in which Pt electrodes with the area of 1 cm^2 were placed with a gap of 5 cm, to measure the ionic conductivity of [BMPy]Tf_2N with various $SiCl_4$ content using impedance analyzer (Electrochemical interface 1287 with frequency response analyzer 1255, Solartron Analytical) over the frequency range of 1 mHz to 100 kHz with an amplitude of 5 mV.

Morphology and composition of the electrodeposited silicon films were analyzed using a FE-SEM(JSM-6500F, JEOL) attached with EDS. XPS(ULVAC-PHI, Quantera SXM) analysis was used to detect impurities on the deposited Si films and their crystal structures were analyzed with x-ray diffractometer(Rigaku D/MAX-2000).

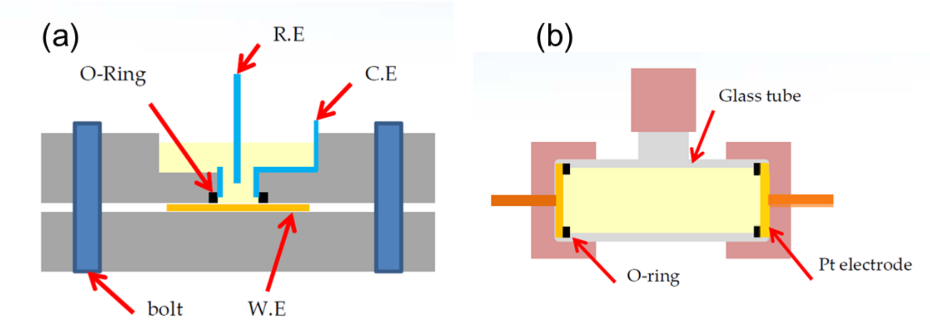

Figure 1. Schematic diagram for (a) electrochemical test cell, and (b) electrochemical impedance spectroscopy.

3. RESULTS AND DISCUSSION

Fig. 2 shows ionic conductivities of [BMPy]Tf_2N with various $SiCl_4$ content. The addition of $SiCl_4$ increased the ionic conductivities of neat [BMPy]Tf_2N ionic liquid, indicating that $SiCl_4$ was not only dissociated into ionic species in [BMPy]Tf_2N, but also decreased the viscosity of the electrolyte compared to the neat ionic liquid. However, ionic conductivities of [BMPy]Tf_2N:$SiCl_4$ system reached a maximum at 0.6 M $SiCl_4$ in the room temperature ionic liquid and then slightly decreased, which might be probably because undissociated $SiCl_4$ after saturation in the ionic liquid increased the viscosity of the electrolyte and decreased its ionic conductivity.

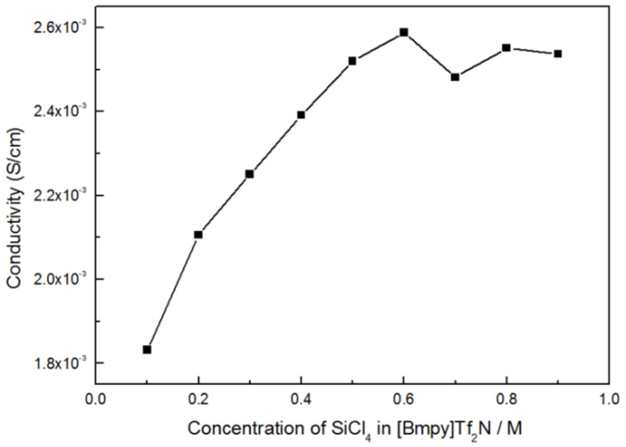

Figure 2. Effect of the content of $SiCl_4$ on the ionnic conductivity of [BMPy]Tf_2N ionic liquid.

Fig. 3 shows linear sweep voltammogram of Au electrode in the [BMPy]Tf_2N with 0.5 M $SiCl_4$. As shown in Fig. 3, linear sweep voltammogram of Au electrode in the pure ionic liquid showed the rise of the current below -2 V, which could be attributed to the breakdown of cation[3,6,19-20], i.e., cathodic reduction of [BMPy] cation. With the addition of $SiCl_4$, the cathodic current of linear sweep voltammogram increased and two cathodic peaks were detected around -0.5 V and -1.3 V(vs. Pt QRE) as shown in Fig. 3. The latter corresponds to the electrodeposition of Si from $SiCl_4$:[BMPy]Tf_2N and the former might be related to the electrochemical reduction of Si species in the electrolyte with their oxidation state from +4 to less positive value. It should be noted that the cathodic decomposition of ionic liquid, which was observed at -1.8 V (vs. Pt QRE) as a peak in the linear voltammogram of Au electrode in the pure ionic liquid, could not be observed in the $SiCl_4$ contained electrolyte up to -2.0 V. These results might be probably due that the deposited Si thin film prevented from the cathodic decomposition of the electrolyte, particularly [BMPy] cation, because the electrodeposition of silicon on the surface of Au electrode changed the electrochemical reactivity of the working electrode with ionic liquid as well as its electronic conductivity from metal to semiconductor, thereby hindering [BMPy] cation to be irreversibly decomposed.

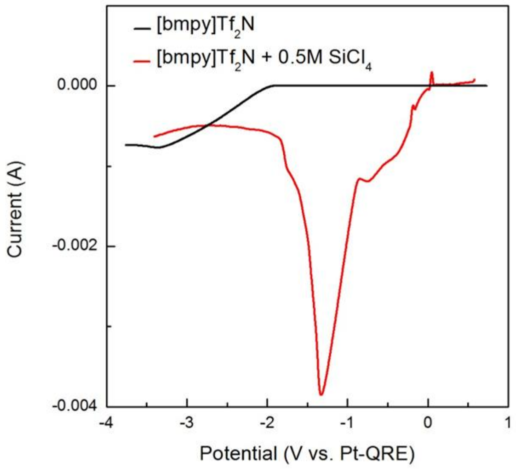

Figure 3. Linear sweep voltammograms of [BMPy]Tf2N and [BMPy]Tf2N with 0.5 M SiCl4 on Au electrode with a scan rate of 10 mV/s.

Fig. 4 and Fig. 5 shows representative linear voltammograms of Cu and Al electrode in [BMPy]Tf_2N with 0.5 M $SiCl_4$, respectively. Fig. 4 and Fig. 5 shows that strong cathodic peak was observed at ~2.4 V(vs. Pt QRE) in the linear sweep voltammograms of Al and Cu electrode, which is much more negative than the decomposition potential of [BMPy] cation as well as the peak related to the reduction of $SiCl_4$ at Au electrode. Therefore, one could not rule out the possibility that decomposition of the ionic liquid simultaneously occurs with the electrodeposition of silicon on these Al and Cu electrode.

In contrast with above-mentioned electrodes, Ag electrode showed far different electrochemical behavior even in the pure ionic liquid (Fig.6). Below 0 V(vs. Pt QRE), a strong reduction peak was observed at ~ 1V (vs. Pt QRE), which might be related to the breakdown of [BMPy] cation in the ionic liquid and is 1V positive than those of Au, Al and Cu electrode. Considering that Ag electrode was already successfully employed as a working electrode for the electrodeposition of Mg in the

RTILs[21], it was unexpected result that Ag electrode showed a narrow electrochemical reductive window in [BMPy]Tf_2N ionic liquid. However, it is no wonder that the electrochemical potential window of the electrolyte would depend on the electrode material. Several research groups already reported the dependency of the electrochemical stability window of RTILs on the electrode materials.[22-24] Zhao et al. reported that the largest potential window was achieved with a glassy carbon electrode, whereas noble metals such as Pt and Au electrodes exhibited smaller reductive potential limits than carbon based electrodes including glassy carbon and boron doped diamond electrode. [23]

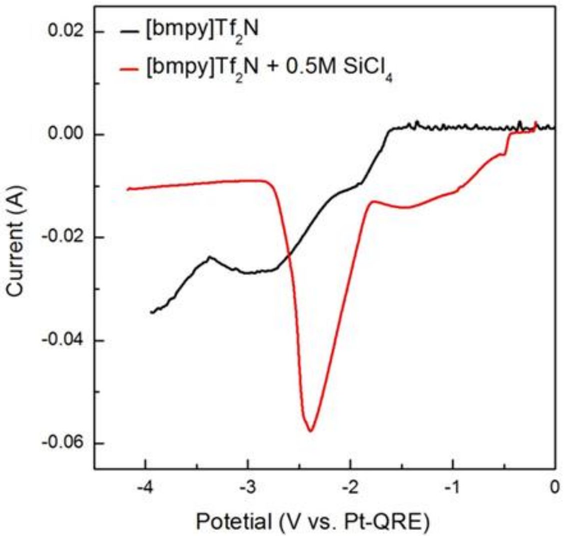

Figure 4. Linear sweep voltammograms of [BMPy]Tf2N and [BMPy]Tf2N with 0.5 M SiCl4 on Cu electrode with a scan rate of 10 mV/s.

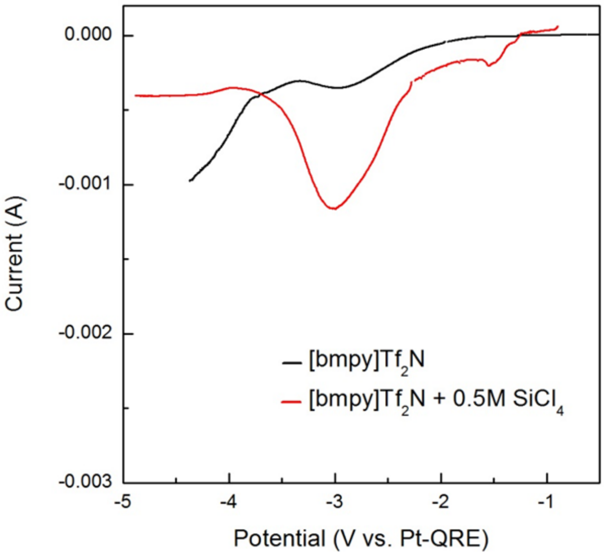

Figure 5. Linear sweep voltammograms of [BMPy]Tf2N and [BMPy]Tf2N with 0.5 M SiCl4 on Al electrode with a scan rate of 10 mV/s.

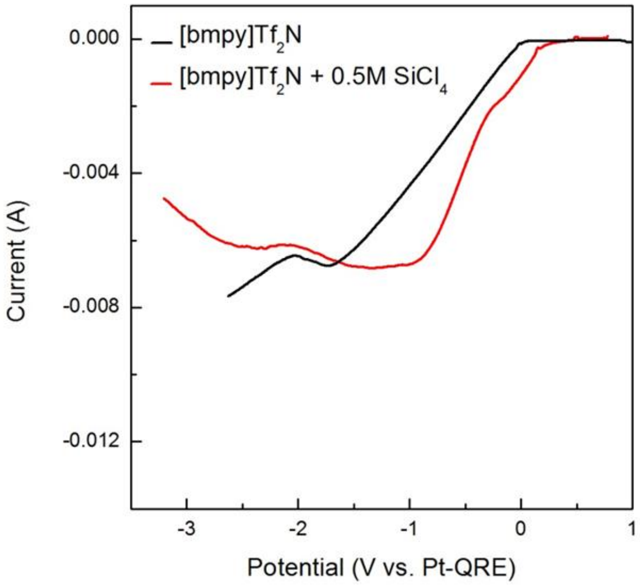

Figure 6. Linear sweep voltammograms of [BMPy]Tf2N and [BMPy]Tf2N with 0.5 M SiCl4 on Ag electrode with a scan rate of 10 mV/s.

They stated that noble metals have a much smaller overpotential for reduction of protons and other impurities in conventional solvent media and the similar situation might be true in aprotic ionic liquids. Although further studies on the electrochemical reduction of [BMPy]Tf_2N ionic liquid on the Ag electrode are needed, smaller cathodic potential limits of Ag electrode might be probably due to the electrochemical reduction of impurities on the Ag electrode.

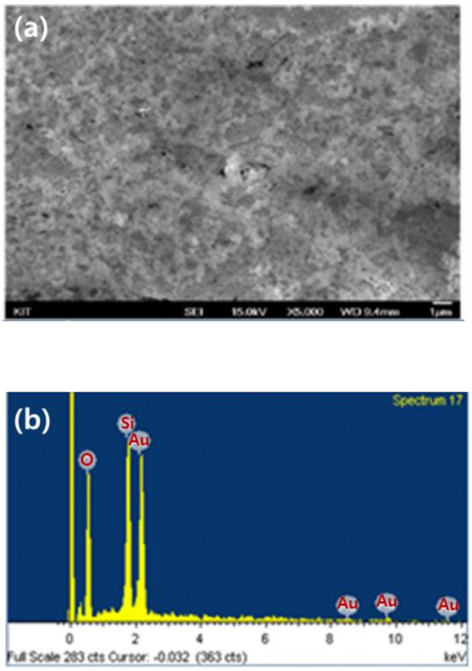

Figure 7. SEM image and EDS result of the electrodeposited film, obtained from the potentiostatic deposition at -1.3 V (vs. Pt QRE) for 1 hour, on the Au electrode

Fig. 7 shows SEM image and EDS result of the electrodeposited film, obtained from the potentiostatic deposition at -1.3 V (vs. Pt QRE) for 1 hour, on the Au electrode from 0.1 M $SiCl_4$: [BMPy]Tf_2N electrolyte. EDS analysis revealed that the electrodeposited film consists of Au, Si and O.

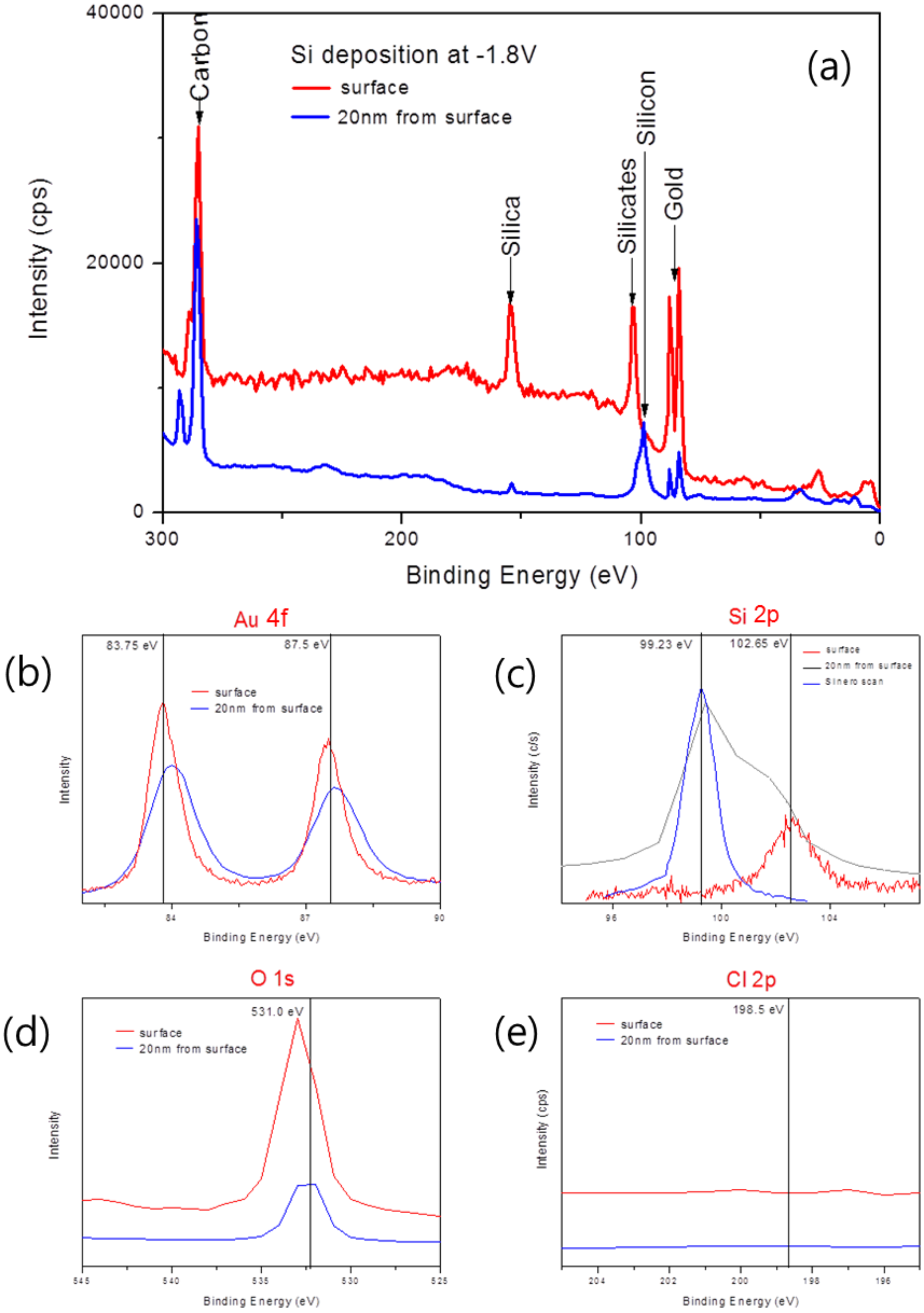

Figure 8. (a) XPS survey scan, (b) Au 4f, (c) Si 2p, (d) O 1s, and (e) Cl 2p of the electrodeposited Si film, obtained from the potentiostatic deposition at -1.8 V (vs. Pt QRE) for 1 hour, on the Au electrode from 0.1 M $SiCl_4$: [BMPy]Tf_2N electrolyte

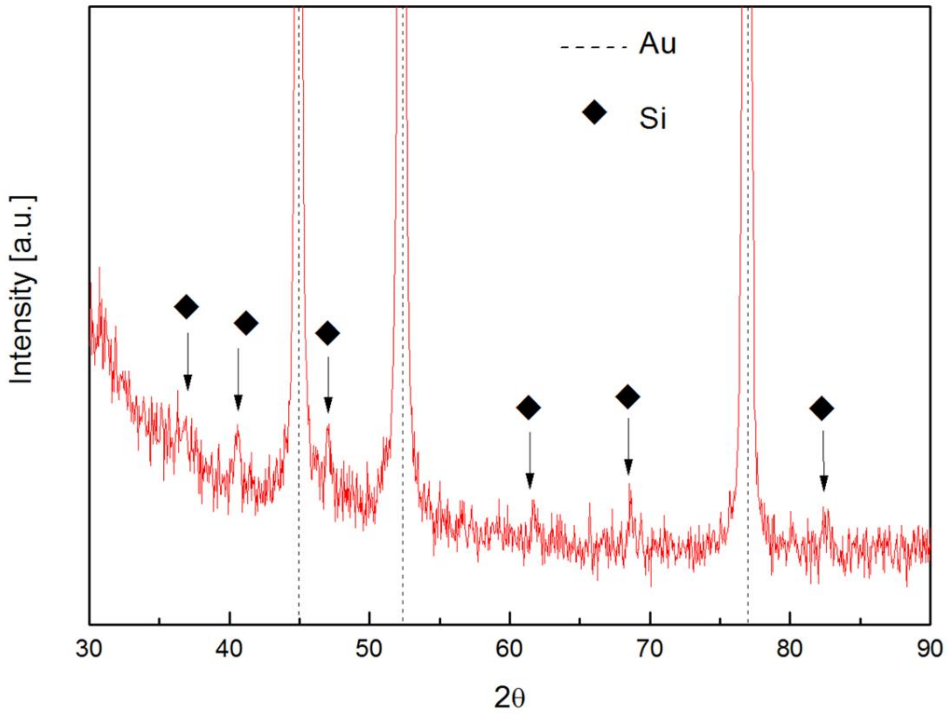

Figure 9. XRD pattern of the electrodeposited Si film, obtained from the potentiostatic deposition at -1.3 V (vs. Pt QRE) for 1 hour, on the Au electrode from 0.1 M $SiCl_4$: $[BMPy]Tf_2N$ electrolyte

In order to analyze the oxidation state of Si in the deposited film, XPS analysis was carried out on the same film. As shown in Fig. 8, the content of silicon was 31.3 % and its binding energy corresponded to that of SiO_2 and other impurities such as chlorine were not detected, implying that surface of the electrodeposited film is mainly SiO_2. However, after the etching of the electrodeposited film using Ar+-ion sputtering, the peak position of Si 2p for the sample shifted toward the binding energy of elemental Si. It indicates that SiO_2 phase of the deposited film might be formed on the surface of the electrodeposited Si film through the oxidation of elemental Si by the exposure to the air. In order to confirm the crystal structure of the electrodeposited Si films, XRD analysis was performed. As shown in Fig. 9, crystalline Si phase with Au substrate were detected from XRD pattern of the sample, indicating that the deposited film consists of polycrystalline Si nanoparticles as a main phase surrounded with amorphous SiO_2 phase. Coupled with these analysis results, it was concluded that Si thin film could be successfully electrodeposited on the Au electrode from $SiCl_4$:$[BMPy]Tf_2N$ electrolyte.

4. CONCLUSION

In this work, we investigated the electrochemical reduction of SiCl4 with a 1-butyl-3-methylpyridinium bis(trifluoromethylsulfonyl) imide($[BMPy]Tf_2N$) room temperature ionic liquid on the various metal electrodes. Linear sweep voltammetry studies of the Au, Al, Cu and Ag electrode showed that the cathodic reduction of the electrolyte was strongly dependent on the working electrode material and the possibility of the electrodeposition of elemental Si. We demonstrated that Si thin film could be obtained on the Au electrode by the potentiostatic reduction, which confirmed by various analytical techniques including x-ray photoelectron spectroscopy, x-ray diffraction and scanning electron microscopy with energy dispersive spectroscopy.

ACKNOWLEDGEMENTS

This study was supported by the R&D Center for Valuable Recycling (Global-Top Environmental Technology Development Program) funded by the Ministry of Environment. (Project No.: GT-11-C-01-140-0)

References

1. A.K. Agrawal, A.E. Austin, *J. Electrochem.Soc.*, 128(1981) 2292.
2. J. Gobet, H. Tannenberger, *J. Electrochem.Soc.*, 135(1988) 109
3. S.Z.E. Abedin, N. Borrissenko, F. Endres, *Electrochem. Comm.*, 6(2004) 510.
4. J.P. Nicholson, *J. Electrochem.Soc.*, 152(2005) C795.
5. N. Borrissenko, S.Z.E. Abedin, F. Endres, *J. Phys. Chem. B*, 110(2006) 6250.
6. R. Al-Salman, S.Z.E. Abedin, F. Endres, *Phys.Chem.Chem.Phys.*, 10(2008) 4650.
7. T. Munisamy, A.J. Bard, *Electrochim. Acta*, 55(2010) 3797.
8. A.L. Bieber, L. Massot, M. Gibilaro, L. Cassayre, P. Taxil, P. Chamelot, *Electrochim. Acta*, 62(2012), 282.
9. M. Bechelany, J. Elias, P. Brodard, J. Michler, L. Phillippe, *Thin Solid Films*(2011), doi:10.1016/j.tsf.2011.09.026.
10. A.L. Bieber, L. Massot, M. Gibilaro, L. Cassayre, P. Chamelot, P. Taxil, *Electrochim. Acta*, 61(2011), 5022.
11. F. Endres, S.Z.E.Abedin, *Phys.Chem.Chem.Phys.*, 8 (2006) 2101.
12. D.R.MacFarlane, M. Forsyth, P. C. Howlett, J. M. Pringle, J. Sun, G. Anant, W. Neil, E.I. Izgorodina, *Acc. Chem. Res.*, 40(2007) 1165
13. D.R. MacFarlane, J. M. Pringle, P.C. Howlett, M. Forsyth, *Phys. Chem. Chem. Phys.*, 12(2010) 1659.
14. J. Mallet, M. Molinari, F. Martineau, F. Delavoie, P. Fricoteaux, M. Troyon, *Nano Lett.*, 8(2008) 3468
15. R. Al-Salman, J. Mallet, M. Molinari, P. Fricoteaux, F. Martineau, M. Troyon, S. Z. E. Abedin ,F. Endres, *Phys.Chem.Chem.Phys.*, 10 (2008) 6233.
16. R. Al-Salman, F. Endres, *J. Mater.Chem.*, 19(2009) 7228
17. S. Eugenio, C. M. Rangel, R. Vilar, S. Quaresma, *Electrochim. Acta*, 28(2011) 10347
18. K. Kwon, J. Park, C. K. Lee, H. Kim, *Int. J. Electrochem. Sci.*, 7(2012) 9835
19. Q.X.Liu, S.Z.E. Abedin, F. Endres, *J. Electrochem.Soc.*, 155(2008) D357
20. A.S. Ismail, S.Z.E. Abedin, O. Hofft, F. Endrres, *Electrochem. Comm.*, 12(2010) 909
21. Y. NuLi, J. Yang, R. Wu, *Electrochem.Comm.*, 7(2005) 1105
22. J. Zhang, A.M. Bond, *Analyst*, 130(2005) 1132
23. C. Zhao, G. Burrell, A.A.J. Torriero, F. Separovic, N.F. Dunlop, D.R. MacFarlane, A. M. Bond, *J. Phys.Chem.B*, 112(2008) 6923.
24. E. I. Rogers, B. Sljukic, C. Hardacre, R.G. Compton, *J.Chem.Eng.Data*, 54(2009) 2049